Pannico et al. Nanoscale Research Letters (2016) 11:315
DOI 10.1186/s11671-016-1539-x

Nanoscale Research Letters

NANO EXPRESS Open Access

Electroless Gold-Modified Diatoms as Surface-Enhanced Raman Scattering Supports

Marianna Pannico[1], Ilaria Rea[2], Soundarrajan Chandrasekaran[3], Pellegrino Musto[1], Nicolas H. Voelcker[3] and Luca De Stefano[2*]

Abstract

Porous biosilica from diatom frustules is well known for its peculiar optical and mechanical properties. In this work, gold-coated diatom frustules are used as low-cost, ready available, functional support for surface-enhanced Raman scattering. Due to the morphology of the nanostructured surface and the smoothness of gold deposition via an electroless process, an enhancement factor for the p-mercaptoaniline Raman signal of the order of 10^5 is obtained.

Keywords: SERS, Diatoms, p-Mercaptoaniline

Background

Surface-enhanced Raman scattering (SERS) is a powerful tool in the fields of analytical chemistry, surface science, electrochemistry, biology, and materials research [1–4]. Its high sensitivity and low detection limit (concentrations of $<10^{-8}$ M), along with reports of single molecule detection, are key advantages that make SERS suitable even in situations where normal Raman spectroscopy fails: Raman scattering signal is usually very weak since its cross section is very low (from 10^3 to 10^6 times weaker than linear Rayleigh scattering); by coupling the electromagnetic field of the incoming probe laser light with the plasmonic field (i.e., surface charge density oscillations of the metal conduction electrons) of the metallic surface, the Raman scattering cross section is greatly enhanced, and therefore also the Raman signal. Moreover, the interaction between molecules under investigation and the metal support could introduce some specific features in the Raman spectrum registered, which can be used for analytical purposes. To obtain appreciable enhancement of Raman scattering, a noble metal surface of nanometer-scale roughness covering macroscopic dimensions area is necessary. Therefore, appropriately prepared substrates are essential to obtain SERS signal enhancement [5–10]. The best signal enhancement factors are currently obtained using silver nanostructured surfaces that unfortunately undergo a sudden oxidation during measurement, making their use as stable supports impractical. In order to overcome material limitations, during the last decade, new classes of artificial materials known as metamaterials and "photonic crystals" and "photonic quasi-crystals" have shown to be very effective SERS substrates, including for applications in biochemical sensing [11, 12]. The production of such optical structures requires a highly specialized design and sophisticated nanoelectronic fabrication techniques, particularly time consuming and costly, such as electron-beam lithography or nanoimprinting, which are not always available in small laboratories. More accessible and cheaper alternative approaches are therefore needed. Diatoms are a group of single-celled photosynthetic algae that possesses microscale shells made of hydrated amorphous silica (SiO_2), called frustules [13]. Frustules show very ornate surface nanoscale pore patterns forming an amazing range of intricate designs with hierarchical ordered dimensions that span from nanoscale to microscale. Due to the quasi-ordered pore patterns, diatoms are endowed with peculiar optical properties including photonic properties, which have been extensively studied in the last few years [14–16]. Unexpected optical properties, due to pores spatial arrangement, such as diffraction-driven self-

* Correspondence: luca.destefano@cnr.it
[2]Institute for Microelectronics and Microsystems, Via P. Castellino 131, Naples 80131, Italy
Full list of author information is available at the end of the article

focusing [17], and gas-sensitive photoluminescence emission, related to material composition, have been demonstrated [18].

In this contribution, we have synthetized, by an innovative method based on electroless deposition of gold, metal-coated diatom frustules that can be exploited as effective supports for SERS.

Methods

The Au plating solution (Oromerse Part B) was purchased from Technic, Inc. (USA). Tin(II) chloride, trifluoroacetic acid, ammonia, methanol, formaldehyde, sodium sulfite, sodium bicarbonate, sulfuric acid, and ethanol were supplied from Sigma-Aldrich (Australia). $AgNO_3$ was obtained from Proscitech (Australia). p-Mercaptoaniline (pMA) 97 % was purchased from Sigma-Aldrich (Italy) and was used without further purification. Diatom frustules of *Aulacoseria* sp. were kindly furnished by Prof. D. Losic, University of Adelaide, Australia.

Diatom frustules were first incubated with hydrogen peroxide solution (35 %) over 24 h to increase the density of oxygen groups on the surface. The electroless Au deposition process includes three steps: sensitization of frustules in a solution of 0.026 M $SnCl_2$ and 0.07 M trifluoroacetic acid for 45 min followed by rinsing in Milli-Q water; activation step, where the sensitized frustules were immersed into a 100-mL ammoniacal solution of 0.029 M $AgNO_3$ for 30 min. During the activation step, a redox reaction helps in the deposition of Ag layer on the sensitized frustules. In the plating/galvanic displacement step, the activated frustules were immersed into a standard prebath solution for 1 h followed by a plating bath for the required deposition time (16–88 h). During this step, the Ag layer was galvanically displaced by Au in the plating bath solution which was kept at approximately 1 °C. The Au layer helps in the further oxidation of formaldehyde and concurrent reduction of Au(I) to Au(0), thus forming multiple layers of Au particles. The plating bath was prepared by mixing Au plating solution (Oromerse Part B, USA) containing 0.079 M $Na_3Au(SO_3)_2$, 0.127 M Na_2SO_3, 0.625 M formaldehyde, and 0.025 M $NaHCO_3$ in Milli-Q water. The pH was adjusted to 8–8.5 using sulphuric acid [19, 20].

Gold-coated frustules were examined by scanning electron microscopy (JEOL JSM-6400) equipped by energy dispersive X-ray analysis (EDAX) spectrometer (Noran Instruments Voyager Series IV).

The Raman spectra of pMA (both spontaneous and surface enhanced) were collected by a confocal Raman spectrometer (Horiba-Jobin Yvon Mod. Labspec Aramis) operating with a diode laser excitation source emitting at 785 nm. The 180° back-scattered radiation was collected by an Olympus metallurgical objective (MPlan 50x, NA = 0.75); a grating with 600 grooves/mm was used throughout. The radiation was focused onto a CCD detector (Synapse Mod. 354308) cooled at −70 °C by a Peltier module. Spectra were registered in the Raman-shift range 800–1800 cm^{-1}. The laser power measured at the output of the objective was 18.7 mW, which resulted in about 17 $mW/\mu m^2$ in terms of power density. The Raman band of a silicon wafer at 520 cm^{-1} was used to calibrate the spectrometer. Collection times were 3 s for non-SERS and 5 s for SERS spectra.

Results and Discussion

The key issue for high-performance SERS substrate is the existence of a uniform, continuous, thin layer of nanocrystalline metal onto the underlying 3D structure: the metal-dielectric interface is essential for both plasmon coupling and repeatable generation of SERS signal. Electroless deposition afforded a high density of Au nanoparticles on frustule surface that acted as preferred sites for further Au nucleation and growth during exposure to the plating solution [21]. The result was a complete coverage of the diatom frustules surface by a nanometric Au film, which completely preserved the original shape of the diatom micro-shell. Secondary electron (SE) images of *Aulacoseira* sp. diatom frustules after electroless deposition are reported in Fig. 1: the cylindrical-shaped frustules were micrometric in size (see Fig. 1a, d; 5–10 μm were total lengths of frustules) and showed ordered lines of nanometric pores (see Fig. 1b, c; 350–370 nm diameters); the outer and inner surfaces were covered by a fine grain Au layer (few nanometers of gold particles strongly interconnected) with some bigger coarse particle agglomerations. The EDAX spectra of the diatoms after electroless deposition confirmed the modified chemical nature of the surface since only the Au characteristic peaks were present in the spectrum reported in Fig. 2. The sensitivity of the SERS sensor based on Au-coated diatoms frustules (Au diatoms) was evaluated by measuring the scattering intensity of p-mercaptoaniline (pMA) probe molecules adsorbed on diatoms. Bonding of pMA to Au surfaces is generally believed to occur via a covalent interaction [22] with hydrogen loss from the thiol group and, therefore, is to be considered a chemisorption rather than a physisorption process. This reactivity produced compact, self-assembled monolayers (SAM) on the substrate surface [23–26]. Before carrying out SERS measurements, the Au-diatom powder was diluted in distilled water and dropped on an optical glass slide. After drying, a 10 μM pMA aqueous solution was dropped on the Au diatoms and dried at room temperature. In the confocal sampling mode, with the adopted objective, a spatial resolution of 1.7 μm^2 is achieved in the *x*-*y* plane. Therefore, single diatoms can be spectroscopically characterized, collecting

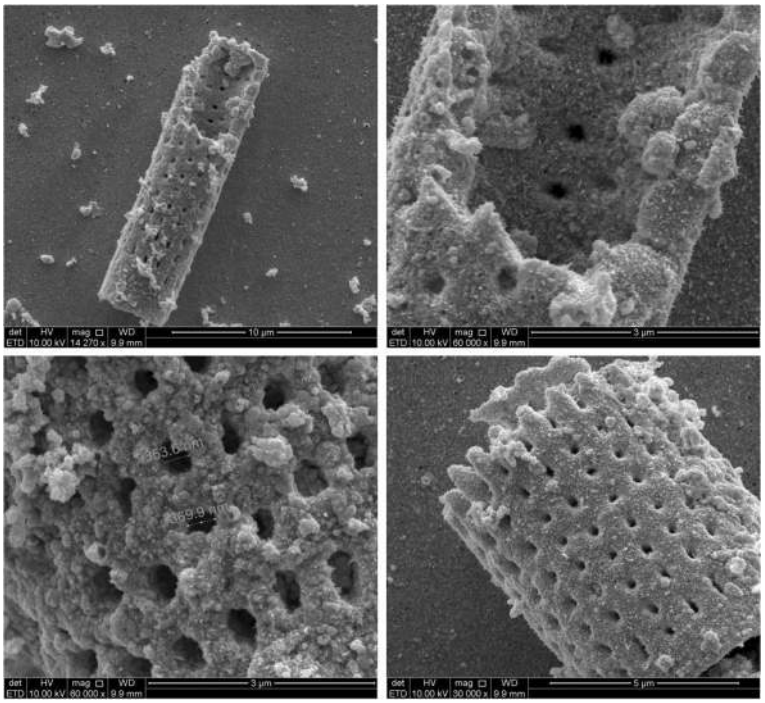

Fig. 1 (**a**, *up left*) Single micrometric diatom frustule. (**b**, *up right*) Au nanoparticle covers homogeneously the outer and inner surfaces of the frustule. (**c**, *down left*) An enlargement of outer surface with pore size measurement. (**d**, *down right*) A smaller micrometric frustule. All images are relative to 48 h of Au deposition time

several spectra in different positions. The resulting SERS spectrum, in the range between 800 and 1800 cm^{-1} is shown in Fig. 3 (blue trace). For comparison, the spontaneous Raman spectrum of pMA powder (red trace in Fig. 3) is also reported. The intensities of the two spectra only seem to be comparable, since the number of molecules that generated the signals was very different. The number of molecules which contribute to the spontaneous Raman scattering ($N_{REF} = 2.55 \times 10^{11}$) was calculated as $N_{REF} = (B_v \times D_{pMA}/M_{pMA}) \times A$, where B_v is the optical excitation volume, D_{pMA} is the density of the pMA crystal at room temperature (1.06 g cm^3), A is the Avogadro number and M_{pMA} is the pMA molecular weight (125.19 g/mol). B_v depends on the Raman operating parameters. It was estimated by carrying out z profile measurements on a silicon substrate under the same operating conditions used for the acquisitions. By varying the focus of the laser on the silicon sample (z profile), the intensity variation of the silicon peak (520 cm^{-1}) shows a Gaussian-type function as shown in Fig. 4. The full width at half maximum (FWHM) gives the waist length of the focal volume ($z = 30.6$ μm), the transverse dimension, x and y (1.28 μm,

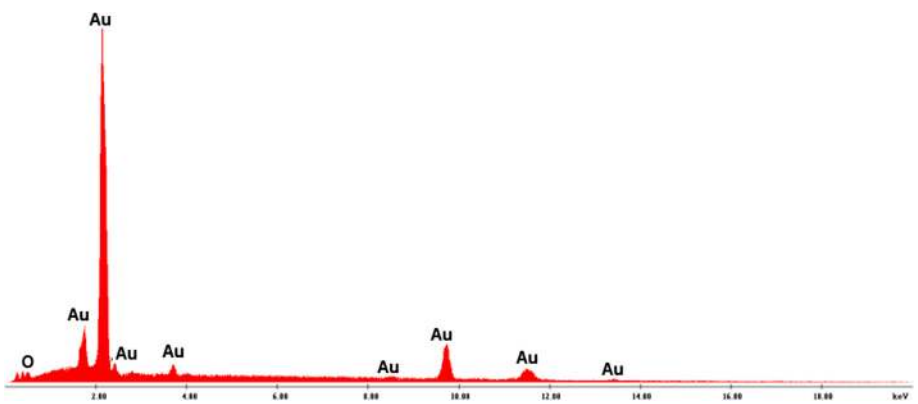

Fig. 2 EDAX signal from diatom surface shows only Au characteristic peaks

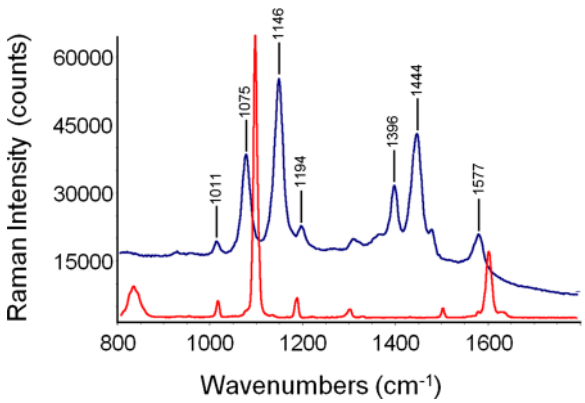

Fig. 3 Raman (*red trace*) and SERS (*blue trace*) spectrum of pMA. The estimated number of sampled molecules is 2.55 × 1011 for the Raman spectrum and 2.90 × 106 for SERS, so that an enhancement factor of about 105 can be estimated

1.28 μm) is determined in view of the numerical aperture of the objective ($N_A = 0.75$) used for the specific wavelength ($\lambda_{LASER} = 785$ nm) according to the relation: $1.22 \times \lambda_{LASER}/N_A$. The resulting B_v is 50.1 μm^3. The number of sampled molecules in the SERS experiment is 2.90×10^6, assuming monolayer formation as reported in literature: thus, the enhancement consists in the fact that populations lower by a factor of around 10^5 produce comparable signals [22, 27].

It was well evident that, beyond the enhancement effect, the SERS spectrum of pMA was more complex than the spontaneous one. In particular, the SERS peaks at 1011, 1075, 1194, and 1577 cm^{-1} supported a direct correspondence with signals observed in the non-resonant pattern, while the three prominent features at 1146, 1395, and 1444 cm^{-1} had not any counterparts in the spontaneous spectrum. The SERS behavior of pMA is complex and still a matter of debate: according to several authors, the new peaks observed in the SERS pattern were due to

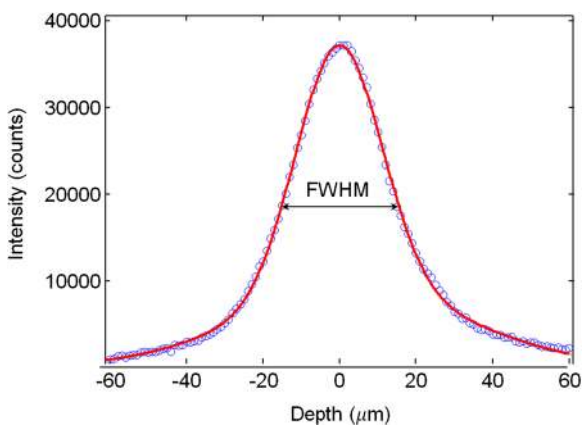

Fig. 4 Depth profile on a silicon wafer to evaluate the sampling volume (Bv)

the dominance of a specific enhancement mechanism (that can be either electromagnetic or charge-transfer mediated) in a given situation and/or to the orientation of the probe with respect to the substrate surface [28–30]. More recently, it was demonstrated that pMA deposited on a roughened Ag surface reacted to form the dimeric form 4,4′-dimercaptoazobenzene (DMAB) under irradiation with a 632-nm laser line [30]. Quantum chemistry calculations performed on the above compound [31] suggested that the intense signals detected at 1143, 1390, and 1432 cm^{-1} on Ag substrates and at 1142, 1390, and 1440 cm^{-1} on Au substrates [32] and previously interpreted as b_2 modes of pMA were in fact a_g modes of the dimeric species. In view of the close similarity of the SERS pattern obtained in the present study with those reported in refs. [33, 34], we concluded that under the experimental conditions of our SERS experiment, the pMA molecule undergone an extensive conversion to DMAB via a catalytic coupling reaction on the metal surface of the Au-diatom system.

SERS spectra collected on different points of the Au-diatom surface are shown in Fig. 5. The average SERS spectrum and the average spectra ± standard deviations are displayed in the inset of Fig. 5.

The SERS spectra consistently presented the same series of peaks, and the intensity ratio between the main peaks was almost constant. The intensity of single peaks changed from point to point meaning that the Au-SERS response was not completely homogeneous. The spectra enhancement achieved demonstrated that Au-diatom-based substrates could be considered good candidates as SERS substrates, but at the same time, their response was not completely reproducible in terms of intensity. In order to characterize the SERS activity of the Au-diatoms substrate, the enhancement factor (EF) was estimated according to the formula:

$$EF = \frac{RS_{EN} \times N_{REF}}{RS_{REF} \times N_{EN}} = 1.0 \times 10^5$$

where RS_{EN} and RS_{REF} are the integrated areas of a specific Raman band (at 1092 cm^{-1} in the reference spectrum and at 1075 cm^{-1} in the SERS) for the SERS and the spontaneous Raman spectrum, respectively [33, 34]. N_{EN} and N_{REF} represent the number of molecules contributing to the SERS and spontaneous Raman scattering, respectively. Assuming total coverage of the sensing surface, the number of molecules contributing to the SERS effect can be estimated as the ratio between the total metal surface illuminated by the laser beam (the transverse dimension) and the geometrical cross section of an individual pMA molecule (0.3 nm^2 per molecule) [35]. However, the morphological analysis evidenced the presence of ordered lines of nanometric pores, which do

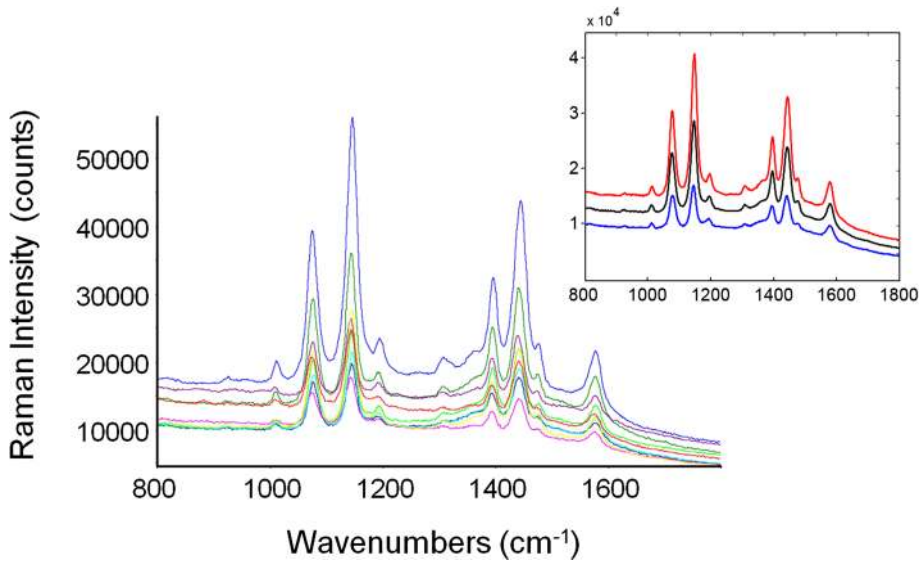

Fig. 5 SERS spectra collected on different points of the Au-diatom surface. The *inset* displays the average SERS spectrum (*black trace*) and the average spectrum ± standard deviation (*blue* and *red traces*)

not contribute to the available surface area. Thus, a filling factor (FF) needed to be multiplied by the total area in order to account for this effect. The FF is defined as

$$\mathrm{FF} = \frac{A_{\mathrm{tot}} - A_v}{A_{\mathrm{tot}}}$$

where A_{tot} and A_v represent, respectively, the total surface area of the diatom and the total area covered by holes. The average FF, estimated from an image analysis of numerous micrographs as that represented in Fig. 2c, was found to be 0.53.

The gold-diatom substrate was intrinsically heterogeneous on a macroscopic scale with respect to the nanometric dimensions of the sensing surface. This was due to the morphology and size of the diatoms. Therefore, a variable SERS response was expected, as a function of the sampling position in a confocal microscopic collection. In fact, as demonstrated in Fig. 5, the overall pattern was highly reproducible but the peak intensity displays a rather wide variation. From the data of Fig. 5, a maximum EF, $\mathrm{EF}_{\mathrm{max}}$ of 1.0×10^5 was estimated, while the average EF value is $(4.6 \pm 2.7) \times 10^4$. It should be highlighted that the above values should be considered as conservative estimates since the dimerization reaction decreased the concentration of pMA and, as a consequence, reduced the intensity of the analytical signal. In summary, the present substrate exhibited reasonably high values of EF, which, coupled with the low cost and the relatively simple preparation process, made them an attractive option for realizing highly sensitive SERS-based detectors.

Conclusions

The efficiency of gold-coated diatoms as SERS substrates was investigated by means of Raman spectroscopy. Gold-coated diatoms were found to be good SERS substrates, enhancing the spontaneous Raman scattering of pMA by a factor of 10^5. SERS spectra collected in different points on the sensing surface showed a reproducible scattering pattern but a relatively large variability in terms of intensity. This effect was due to the intrinsic heterogeneity at a microscale level of the sensing surface. Despite this limitation, gold-coated diatoms substrate may be considered a low-cost, easy to prepare, and very promising for analytical applications.

Competing Interests

The authors declare that they have no competing interests.

Authors' Contributions

LDS and NHV planned the experiment. SC and NHV modified diatoms. MP and PM measured and commented Raman spectra. MP, IR, and LDS analyzed data and wrote the paper. All authors corrected and approved the paper.

Author details

[1]Institute for Polymers, Composite and Biomaterials, Pozzuoli, NA, Italy. [2]Institute for Microelectronics and Microsystems, Via P. Castellino 131, Naples 80131, Italy. [3]Future Industries Institute, University of South Australia, Mawson Lakes Blvd, Adelaide, Australia.

Received: 18 March 2016 Accepted: 24 June 2016
Published online: 29 June 2016

References

1. Campion A, Kambhampati P (1998) Surface-enhanced Raman scattering. Chem Soc Rev 27:241–250
2. Oklejas V, Sjostrom C, Harris JM (2002) SERS detection of the vibrational Stark effect from nitrile-terminated SAMs to probe electric fields in the diffuse double-layer. J Am Chem Soc 124(11):2408–2409

3. Shafer-Peltier KE, Haynes CL, Glucksberg MR, Van Duyne RP (2003) Toward a glucose biosensor based on surface-enhanced Raman scattering. J Am Chem Soc 125(2):588–593
4. Cao YWC, Jin RC, Mirkin CA (2002) Nanoparticles with Raman spectroscopic fingerprints for DNA and RNA detection. Science 297(5586):1536–1540
5. Smith DR, Padilla WJ, Vier DC, Nemat-Nasser SC, Schultz S (2008) Composite medium with simultaneously negative permeability and permittivity. Phys Rev Lett 4:4184–4187
6. Vardeny ZV, Nahat A, Agrawal A (2013) Optics of photonic quasicrystals. Nat Photon 7:177–187
7. Alvarez-Puebla RA et al (2015) Special issue on surface-enhanced Raman spectroscopy. J Optics 17(11):110201
8. Dal Negro L, Boriskina S (2012) Deterministic aperiodic nanostructures for photonics and plasmonics applications. Laser Photonics Rev 6:178–218
9. Rippa M, Capasso R, Mormile P, De Nicola S, Zanella M, Manna L, Nenna G, Petti L (2013) Bragg extraction of light in 2D photonic thue-morse quasicrystal patterned in active CdSe/CdS nanorods-polymer nanocomposites. Nanoscale 5(1):331–336
10. Petti L, Rippa M, Zhou J, Manna L, Zanella M, Mormile P (2011) Novel hybrid organic/inorganic 2D quasiperiodic PC: from diffraction pattern to vertical light extraction. Nanoscale Res Lett 6:371–376
11. Fang C, Ellis AV, Voelcker NH (2012) Electrochemical synthesis of silver oxide nanowires, microplatelets and application as SERS substrate precursors, electrochim. Acta 59:346–353
12. Cheng F, Bandaru M, Ellis A, Voelcker NH (2013) Beta-cyclodextrin decorated nanostructured SERS substrates facilitate selective detection of endocrine disruptor chemicals. Biosens Bioelectron 42:632–639
13. De Stefano M, De Stefano L (2005) Nanostructures in diatom frustules: functional morphology of valvocopulae in Cocconeidacean monoraphid taxa. J Nanosci Nanotechnol 5:15–24
14. Losic D, Pillar RJ, Dilger T, Mitchell JG, Voelcker NH (2007) Atomic force microscopy (AFM) characterization of the porous silica nanostructure of two centric diatoms. J Porous Mat 14:61–69
15. De Tommasi E, Rea I, Mocella V, Moretti L, De Stefano M, Rendina I, De Stefano L (2010) Multi-wavelength study of light transmitted through a single marine centric diatom. Opt Exp 18(12):12203–12212
16. De Tommasi E, De Luca AC, Lavanga L, Dardano P, De Stefano M, De Stefano L, Langella C, Rendina I, Dholakia K, Mazilu M (2014) Biologically enabled sub-diffractive focusing. Opt Exp 22(22):27214–27227
17. Ferrara MA, Dardano P, De Stefano L, Rea I, Coppola G, Rendina I, Congestri R, Antonucci A, De Stefano M, De Tommasi E (2014) Optical properties of diatom nanostructured biosilica in Arachnoidiscus sp: micro-optics from Mother Nature. PLoS One 9(7):e103750. doi:10.1371/journal.pone.0103750
18. Bismuto A, Setaro A, Maddalena P, De Stefano L, De Stefano M (2008) Marine diatoms as optical chemical sensors: a time resolved study. Sens Actuators B: Chem 130(1):396–399
19. Losic D, Mitchell JG, Voelcker NH (2006) Fabrication of gold nanostructures by templating from porous diatom frustules. New J Chem 6:908–914
20. Yu Y, Addai-Mensah J, Losic D (2010) Synthesis of self-supporting gold microstructures with three-dimensional morphologies by direct replication of diatom templates. Langmuir 26(17):14068–14072
21. Menon VP, Martin CR (1995) Fabrication and evaluation of nanoelectrode ensembles. Anal Chem 67:1920–1928
22. Mohri N, Matsushita S, Inoue M, Yoshikawa K (1998) Desorption of 4-aminobenzenethiol bound to a gold surface. Langmuir 14:2343–2347
23. Wang H, Levin CS, Halas NJ (2005) Nanosphere arrays with controlled sub-10-nm gaps as surface-enhanced raman spectroscopy substrates. J Am Chem Soc 127:14992–14993
24. Jiao LS, Wang Z, Shen LNJ, You TY, Dong SJ, Ivaska A (2006) In-situ electrochemical SERS studies on electrodeposition of aniline on 4-ATP/Au surface. J Solid State Interact 10:886–893
25. Oldenburg SJ, Westcott SL, Averitt RD, Halas NJ (1999) Surface enhanced Raman scattering in the near infrared using metal nanoshell substrates. J Chem Phys 111:4729–4736
26. Boettcher CJF (1973) Theory of electric polarization, vol 1. Elsevier Scientific Publishing, Amsterdam, pp 74–82
27. Cheng F, Brodoceanu D, Kraus T, Voelcker NH (2013) Templated silver nanocube arrays for single-molecule SERS detection. RSC Advances 3:4288–4293
28. Osawa M, Matsuda N, Yoshii K, Uchida I (1994) Charge transfer resonance raman process in surface-enhanced raman scattering from p-aminothiophenol adsorbed on silver: Herzberg-Teller contribution. J Phys Chem 98:12702–12707
29. Hu XG, Wang T, Wang L, Dong SJ (2007) Surface-enhanced Raman scattering of 4-aminothiophenol self-assembled monolayers in sandwich structure with nanoparticle shape dependence: off-surface plasmon resonance condition. J Phys Chem C 111:6962–6969
30. Uetsuki K, Verma P, Yano T, Saito Y, Ichimura T, Kawata S (2010) Experimental identification of chemical effects in surface enhanced Raman scattering of 4-aminothiophenol. J Phys Chem C 114:7515–7520
31. Maniu D, Chis V, Baia M, Toderas F, Astilean S (2007) Density functional theory investigation of p-aminothiophenol molecules adsorbed on gold nanoparticles. J Optoelectron Adv M 9:733–736
32. Huang YF, Zhu HP, Liu GK, Wu DY, Ren B, Tian ZQ (2010) When the signal is not from the original molecule to be detected: chemical transformation of para-aminothiophenol on Ag during the SERS measurement. J Am Chem Soc 132:9244–9246
33. Fang Y, Li Y, Xu H, Sun M (2010) Ascertaining p, p′-dimercaptoazobenzene produced from p-aminothiophenol by selective catalytic coupling reaction on silver nanoparticles. Langmuir 26:7737–7746
34. Shin KS (2008) Effect of surface morphology on surface-enhanced Raman scattering of 4-aminobenzenethiol adsorbed on gold substrates. J Raman Spectrosc 39:468–473
35. Marquestaut N, Martin A, Talaga D, Servant L, Ravaine S, Reculusa S, Bassani DM, Gillies E, Lagugné-Labarthet F (2008) Raman enhancement of azobenzene monolayers on substrates prepared by Langmuir–Blodgett deposition and electron-beam lithography techniques. Langmuir 24(19):11313–11321